Harnessing Plasticity in an Amine-Borane as a Piezoelectric and Pyroelectric Flexible Film

Zhang, Yan; Hopkins, Margaret A.; Liptrot, David J.; Khanbareh, Hamideh; Groen, Pim; Zhou, Xuefan; Zhang, Dou; Bao, Yinxiang; Zhou, Kechao; Bowen, Chris R.

DOI
10.1002/anie.202001798

Publication date
2020

Document Version
Final published version

Published in
Angewandte Chemie - International Edition

Energy Conversion

How to cite:
International Edition: doi.org/10.1002/anie.202001798
German Editon: doi.org/10.1002/ange.202001798

Harnessing Plasticity in an Amine-Borane as a Piezoelectric and Pyroelectric Flexible Film

Yan Zhang, Margaret A. Hopkins, David J. Liptrot, Hamideh Khanbareh, Pim Groen, Xuefan Zhou, Dou Zhang, Yinxiang Bao, Kechao Zhou, Chris R. Bowen,* and David R. Carbery**

Dedicated to the memory of Dr. Matt John

Abstract: *We demonstrate that trimethylamine borane can exhibit desirable piezoelectric and pyroelectric properties. The material was shown to be able operate as a flexible film for both thermal sensing, thermal energy conversion and mechanical sensing with high open circuit voltages (>10 V). A piezoelectric coefficient of $d_{33} \approx 10$–$16\ pC\,N^{-1}$, and pyroelectric coefficient of $p \approx 25.8\ \mu C\,m^{-2}\,K^{-1}$ were achieved after poling, with high pyroelectric figure of merits for sensing and harvesting, along with a relative permittivity of $\varepsilon_{33}^{\sigma} \approx 6.3$.*

The identification and development of materials which exhibit plasticity[1] and mechanical flexibility[2] is an emergent design principle in the area of piezo- and pyro-electric materials for the creation of future smart sensors and transducers. A useful qualitative view of plastic crystals is one where a solid lattice retains positional ordering of the component units, such as ions or molecules, yet with rotational disorder of these units. Typically, this qualitative model is consistent with the fact that the components of plastic crystals tend to display high levels of symmetry, often with spheroidal three-dimensional shapes. A prototypical example is the tetrahedral non-polar molecule neopentane (tetramethylmethane).

In this report we seek to apply and expand upon specific concepts of medicinal discovery chemistry, whereby the function of molecules to be developed is bioactivity. In organic molecular functional materials, the function is different, including the aim to achieve a piezoelectric or pyroelectric response. However, the need to re-evaluate, discover and develop molecules to maximise such useful properties is common to both contexts. One design tool used in medicinal chemistry is that is the isostere, where the molecules are designed to retain analogous molecular shape and size, yet, by utilizing atomic components the molecule is able to exhibit new or enhanced properties, for example, increased polarity.

B-N fragments have received increasing interest in the last two decades as isosteres for C–C moieties. Alongside isosterism, boron's origin in the icosagens (3 valence electrons) and nitrogen's place in the pnictogens (5 valence electrons) renders the B–N functional group isoelectronic to its 8-electron C–C analogue. The introduction of a B–N group has been shown to have profound effects on molecular and solid-state electronic and optical properties of systems, a consequence of the effect of their introduction upon the frontier orbitals of such species. Alongside these effects, the electronegativities of boron and nitrogen render B–N fragments highly polar and can introduce the potential for new intramolecular interactions. Ammonia borane, the B–N analogue of ethane is a solid at room temperature and decomposes with the loss of dihydrogen upon heating in preference to undergoing a change of phase, physicochemical properties proposed to originate from $NH^{\delta+}\cdots H^{\delta-}B$ interactions.

Neopentane is recognized as a plastic crystalline material,[3] and a key consideration in this work is to develop materials which not only offer excellent response but are also not reliant on the single crystal morphologies being studied. Recently, it has been recognised that the incorporation of multi-axiality of the constituent molecular building block can assist in achieving thin film morphologies which are not reliant on complex preparation strategies or single crystal morphology.[4] Our strategy to enable the insertion of polar character to neopentane is the replacement of a single C–C σ-bond with a charge-separated N^{+}–B^{-} σ-bond, that is in the first instance to examine trimethylamine borane, TMAB (Figure 1).[5]

TMAB has a rich pedigree in researchers assessing the level of disorder in the solid state. For example, microwave spectroscopy[6] solid-state NMR,[7] and X-ray diffraction[8] has examined dipole and bond lengths in TMAB. Significantly,

[*] Dr. Y. Zhang, X. Zhou, Prof. D. Zhang, Y. Bao, Prof. K. Zhou
State Key Laboratory of Powder Metallurgy, Central South University
Changsha, Hunan, 410083 (China)
Dr. Y. Zhang, Dr. M. A. Hopkins, Dr. H. Khanbareh, Prof. C. R. Bowen
Department of Mechanical Engineering, University of Bath
Claverton Down, Bath BA2 7AY (UK)
E-mail: c.r.bowen@bath.ac.uk
Dr. D. J. Liptrot, Dr. D. R. Carbery
Department of Chemistry, University of Bath
Claverton Down, Bath BA2 7AY (UK)
E-mail: d.j.liptrot@bath.ac.uk
d.carbery@bath.ac.uk
Prof. P. Groen
Novel Aerospace Materials Group, Faculty of Aerospace Engineering,
Delft University of Technology
Kluyverweg 1, Delft (The Netherlands)
Supporting information and the ORCID identification number(s) for the author(s) of this article can be found under https://doi.org/10.1002/anie.202001798.

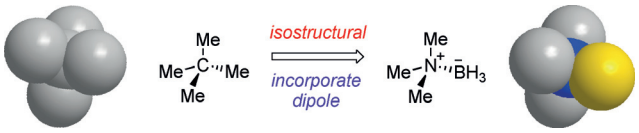

Figure 1. Design principle: to retain molecular shape yet incorporate an effective dipole.

the crystallographic study of TMAB reports the crystallisation of this material in the polar space group, *R3m*.

Mechanical pressing of the material forms a submillimeter thick film,[5b] which is observed to produce SHG proficiently across the material. PXRD analysis of the film implies a degree of crystallinity (Figure S3), showing peaks consistent with those predicted from the single crystal diffraction data for TMAB.

Figure 2 shows the relative permittivity and piezoelectric responses of pressed films of TMAB after poling. Due to a small degree of electrical conductivity at room temperature (RT, 25 °C), a frequency dependent permittivity can be observed at low frequencies (< 200 Hz), Figure S4, while the permittivity is more frequency independent at higher frequencies (> 400 Hz). This is a common phenomenon in dielectrics which follows the universal dielectric response.[9] As the temperature is reduced, from RT to −60 °C the frequency dependence is reduced, due to the reduced AC conductivity, see Figure S5, with a calculated activation energy $E_{ac} \approx 0.287$ eV in Figures S5 and S6.

With a decrease of temperature from RT to −60 °C, the relative permittivity under constant stress $(\varepsilon^{\sigma}_{33})$ at 1 kHz decreased from $\varepsilon^{\sigma}_{33} \approx 6.3$ to $\varepsilon^{\sigma}_{33} \approx 2.1$, as shown in Figure 2a. The measured piezoelectric d_{33} coefficient of TMAB with poling temperature is also shown in Figure 2a. The piezoelectric coefficient was $d_{33} \approx 10$–$16\ \mathrm{pC\,N^{-1}}$ when the poling temperature was higher than −40 °C.

However, no piezoelectric response ($d_{33} = 0\ \mathrm{pC\,N^{-1}}$) could be observed when the poling temperature was reduced to −60 °C, where the dipoles can be considered as frozen.

This observation is consistent with the observed decrease in the relative permittivity to $\varepsilon^{\sigma}_{33} \approx 2.1$ when the temperature reached −60 °C in Figure 2a, which could be a result of a phase change at this low temperature.

Piezo Force Microscopy (PFM) was used to explore the dipole switching behaviour of the material using a + 12 V and −12 V dc bias, where a clear butterfly-shaped and 180° phase switching hysteresis loop can be observed in Figures 2b and c, which agrees with the good piezoelectric d_{33} after poling.

As indicated by Liu et al., ionic dynamics or an electret-like response cannot be excluded,[10] although no switching behaviour was observed when a non-ferroelectric polydimethylsiloxane (PDMS) sample was subjected to a similar testing regime, see Figure S7. An evaluation of the bulk polarisation-electric field response in pressed discs was less conclusive, as shown in Figure S8, which indicates that on a larger scale sample there is a contribution from conductivity, as in the frequency dependent permittivity data of Figure S4.

In addition to piezoelectric properties, which originate from a change in polarisation with stress, the pyroelectric properties were also evaluated which are a result of a change

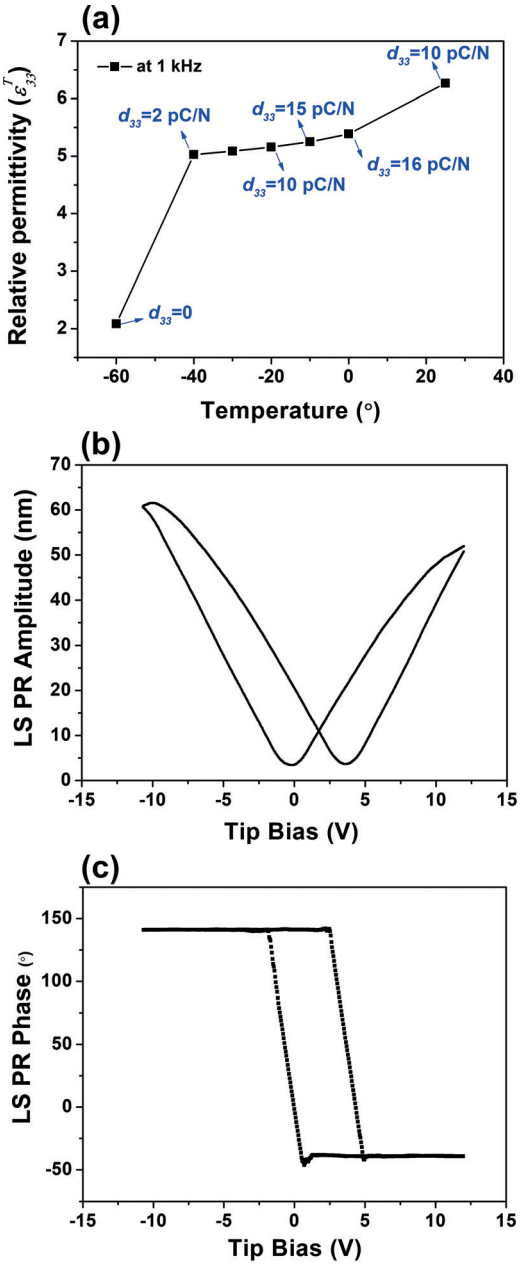

Figure 2. a) Relative permittivity at 1 kHz with temperature. Piezo Force response of a pressed film: b) amplitude–voltage response, c) phase–voltage response.

in polarisation with temperature. Figure S9 shows the temperature oscillation that was subjected to the poled material and the resulting pyroelectric current. The pyroelectric current (I_p) is given by,

$$I_p = p\,A\,(\mathrm{d}T/\mathrm{d}t) \tag{1}$$

where p is the pyroelectric coefficient normal to the electrodes ($\mathrm{C^{-1}\,m^{-2}\,K^{-1}}$), A is material area ($\mathrm{m^2}$) and $\mathrm{d}T/\mathrm{d}t$ is the rate of temperature change ($\mathrm{K\,s^{-1}}$). This method is based on the fact that the pyroelectric current is directly proportional to $\mathrm{d}T/\mathrm{d}t$, while the thermally stimulated non-pyroelectric current is either constant or proportional to the temperature.[11]

When the sample is heated with a small sinusoidal temperature wave, an AC current is produced by the sample. The amplitude and phase of the current define the ratio of pyroelectric and non-pyroelectric currents. The AC component, which is in phase with the temperature wave, is the non-pyroelectric current. However, if the AC component precedes the temperature wave by 90°, the origin is a pyroelectric current. In Figure 3a, the pyroelectric current and phase difference between the temperature (T) and current (I) are shown for three samples of various polarisation states, thus different piezoelectric d_{33} coefficients. The phase angle of of $\theta \approx 90°$ for all samples is indicative of the current being pyroelectric in origin, since no current is observed when $dT/dt \approx 0$ [as in Eq. (1)]. The pyroelectric current also rises with frequency, and dT/dt, as also expected from Equation (1). Materials with high piezoelectric d_{33} coefficient exhibit the highest pyroelectric current, see Figure S9, indicating that both the piezoelectric and pyroelectric response are linked to the remnant polarisation of the materials. The stability of the current during thermal cycling, as seen in Figure S9, is also an indicator that it is pyroelectric in origin and results from the redistribution of compensation charge during polarisation changes with temperature;[12] if the current had originated from trapped charges induced by the poling process, the release of such charges during cycling would lead to a gradual decay of current. The calculated pyroelectric coefficient, shown in Figure 3b, increases with increasing piezoelectric d_{33} coefficient and was frequency independent, indicating a pure pyroelectric behaviour, with a $p \approx 25.8\ \mu C\,m^{-2}K^{-1}$ and is comparable to polymer ferroelectrics, such as polyvinylidene difluoride (PVDF); as seen in Table 1.

The pyroelectric figures of merit for voltage sensitivity, $F_V = \frac{p}{\varepsilon_0 \varepsilon_{33}^{\sigma} C_E}$ and thermal harvesting $F'_E = \frac{p^2}{\varepsilon_0 \varepsilon_{33}^{\sigma} (C_E)^2}$[13] were $0.26\ m^2C^{-1}$ and $3.58\ pm^3J^{-1}$, respectively; where C_E is the specific heat capacity. A comparison of other common pyroelectrics are shown in Table 1, and indicates competitive performance.

To verify the potential of the material in a real device, a periodic thermal fluctuation was applied to the sample by an IR lamp, where the open circuit voltage and short circuit current with temperature change are provided in Figure S6.

The poled TMAB disk was utilised to charge a capacitor with a capacitance $C = 4.2\ \mu F$ and the voltage across the storage capacitor was monitored as it charged with the pyroelectric energy harvester via a full-wave bridge rectifier, as shown in Figure 4d.

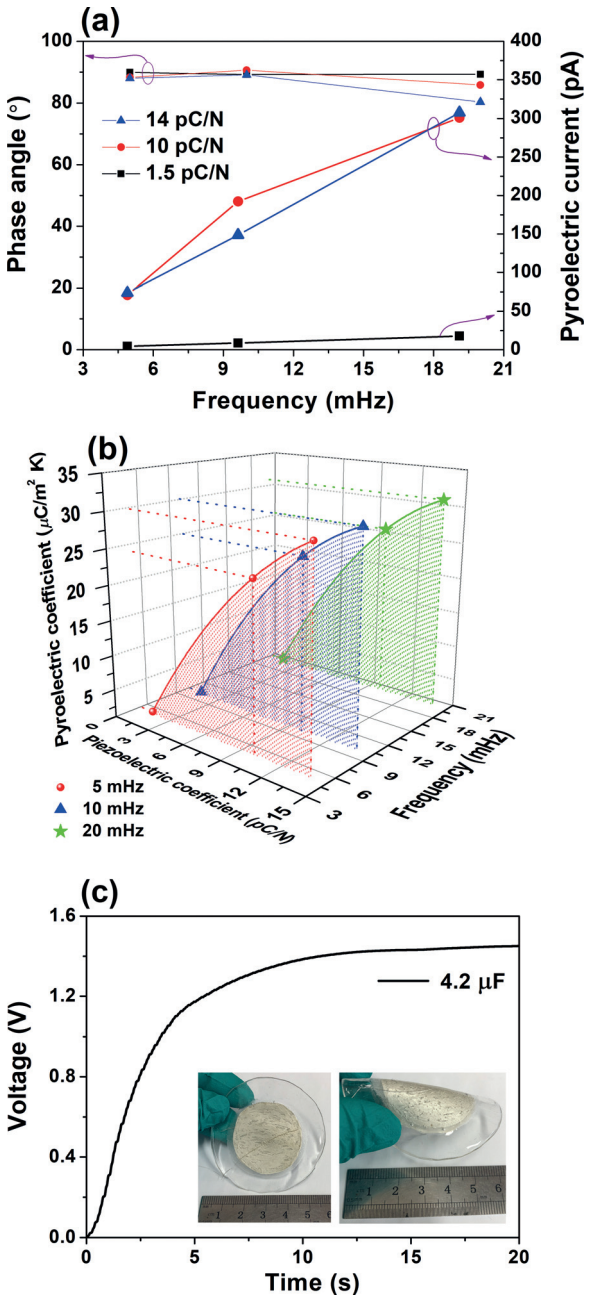

Figure 3. Pyroelectric response a) response of current in closed circuit mode, b) estimation of pyro-coefficient, c) charging curve of the 4.2 μF capacitor using the pyroelectric borane.

Table 1: Comparison of key properties of materials at room temperature including polyvinylidene difluoride (PVDF), lead zirconate titanate (PZT).

Material	Relative permittivity, 1 kHz	Specific heat capacity (C_E) [$J\,cm^{-3}\,K^{-1}$]	Pyro-coefficient (p) [$\mu C\,m^{-2}\,K^{-1}$]	$F'_E = \frac{p^2}{\varepsilon_0 \varepsilon_{33}^{\sigma} (C_E)^2}$ [$pm^3\,J^{-1}$][a]	Figure of merit $F_V = \frac{p}{\varepsilon_0 \varepsilon_{33}^{\sigma} C_E}$ [$m^2\,C^{-1}$]	Figure of merit $F_I = \frac{p}{C_E}$ [$pm\,V^{-1}$]
TMAB	6	1.87	25.8	3.58	0.26	13.80
PVDF[14]	6–12	2.43	33	1.16[b]	0.15	13.58
PZT[15]	2100	2.5	390	1.31[b]	0.008	156
$BaTiO_3$[14a,16]	1200	2.6	200	0.56[b]	0.007	76.92

[a] ε_0 is the permittivity of free space, where $\varepsilon_0 \approx 8.85\ pF\,m^{-1}$.[13] [b] Estimated calculation based on the experimental data reported.

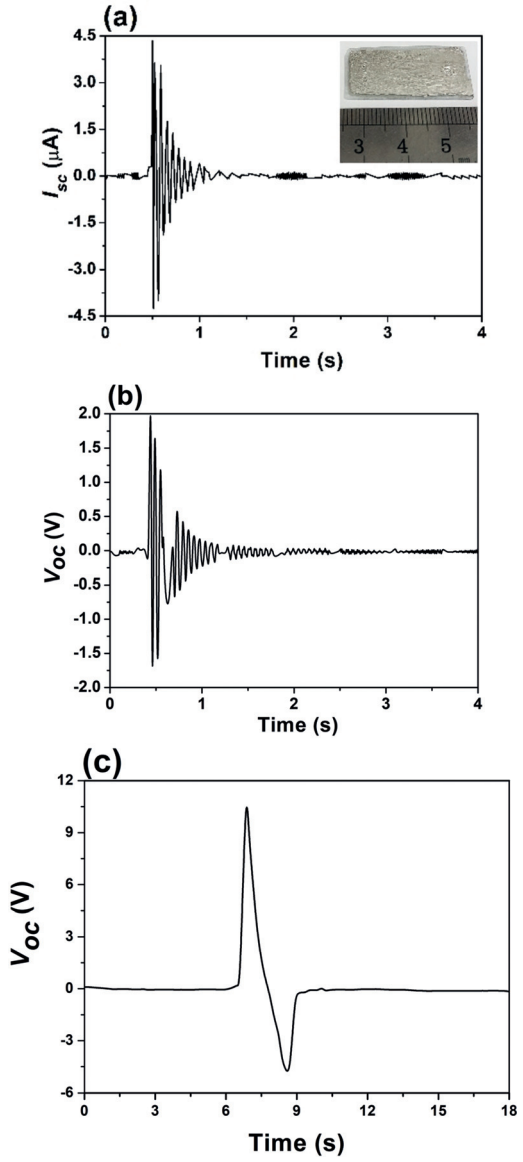

Figure 4. Piezoelectric sensing response via mechanical excitation with the output of a) short-circuit current; b) open circuit voltage. c) Piezoelectric sensing performance via finger tapping with the output of open circuit voltage.

Within a time of 12 s, sufficient charge was generated to increase voltage on the capacitor from 0 V to 1.4 V, which was able to store 4.116 μJ of energy E, based on $E = 0.5\,CV^2$, where V is the saturation voltage during charging.

While Figure 3c, demonstrates the material as a pyroelectric device, Figure 4 demonstrates its ability to operate as a piezoelectric sensor when subjected to mechanical oscillation. The material was bonded to a cantilever beam (Figure S11) which was subjected to a mechanical impulse to oscillate the beam leading to vibration which gradually decayed with time due to damping. As can be seen from Figures 4a and b, a 4.46 μA short-circuit current and 1.98 V open-circuit voltage were initially generated, and both the current and voltage decreased as the vibration of the cantilever subsequently decayed with time. When the poled material was used as a stand-alone sensor and was subjected to a single mechanical impact by a finger, as shown in the inset of Figure S12, a positive polarity short circuit current ($\approx$0.42 μA, Figure S12) and open circuit voltage ($\approx$10.85 V, Figure 3c) were detected which was followed by current and voltage of opposing polarity as the pressure was released and compensation charges flowed in the opposite direction.

Similarly, capacitor charging performance can be conducted to evaluate its piezoelectric energy harvesting ability by the utilisation of a shaker under the application of frequency.[17]

In summary, we have shown trimethylamine borane can exhibit attractive piezoelectric and pyroelectric properties when subjected to a poling for operation with piezoelectric coefficients of $d_{33} \approx 10$–$16\ \mathrm{pC\,N^{-1}}$, relative permittivity of $\varepsilon_{33}^{\sigma} \approx 6.3$, pyroelectric coefficient $p \approx 25.8\ \mu\mathrm{C\,m^{-2}\,K^{-1}}$ with high pyroelectric figures of merit. The material exhibits second harmonic generation and switching via piezo-force microscopy, and was shown to be able operate as a flexible film for both thermal sensing/conversion, and mechanical sensing with high open circuit voltages (>10 V). These desirable properties, which were identified originating from a medicinal chemistry design-mimetic process, firmly suggest that optimisation approaches including isosterism have much to contribute to the targeting of functions beyond bioactivity.

Acknowledgements

D.J.L. acknowledges the Royal Society for the support of a University Research Fellowship. D.R.C. thanks the EPSRC (grant EP/K004956/1).

Conflict of interest

The authors declare no conflict of interest.

Keywords: energy conversion · flexible films · main group elements · piezoelectricity · pyroelectricity

How to cite: *Angew. Chem. Int. Ed.* **2020**, *59*, 7808–7812
Angew. Chem. **2020**, *132*, 7882–7886

[1] a) J. Timmermans, *J. Chim. Phys.* **1938**, *35*, 331–344; b) J. Harada, Y. Kawamura, Y. Takahashi, Y. Uemura, T. Hasegawa, H. Taniguchi, K. Maruyama, *J. Am. Chem. Soc.* **2019**, *141*, 9349–9357; c) J. Harada, N. Yoneyama, S. Yokokura, Y. Takahashi, A. Miura, N. Kitamura, T. Inabe, *J. Am. Chem. Soc.* **2018**, *140*, 346–354.

[2] T. Vijayakanth, A. K. Srivastava, F. Ram, P. Kulkarni, K. Shanmuganathan, B. Praveenkumar, R. Boomishankar, *Angew. Chem. Int. Ed.* **2018**, *57*, 9054–9058; *Angew. Chem.* **2018**, *130*, 9192–9196.

[3] R. Rey, *J. Phys. Chem. B* **2008**, *112*, 344–357.

[4] Y.-Y. Tang, P.-F. Li, W.-Q. Liao, P.-P. Shi, Y.-M. You, R.-G. Xiong, *J. Am. Chem. Soc.* **2018**, *140*, 8051–8059.

[5] a) A. Staubitz, A. P. M. Robertson, M. E. Sloan, I. Manners, *Chem. Rev.* **2010**, *110*, 4023–4078; b) During the review process for this article, the following work on the solid state properties of TMAB was published: C. M. Reddy, A. Mondal, B. Bhatta-

charya, S. Das, S. Bhunia, R. Chowdhury, S. Dey, *Angew. Chem. Int. Ed.* **2020**, https://doi.org/10.1002/anie.202001060; *Angew. Chem.* **2020**, https://doi.org/10.1002/ange.202001060.
[6] P. Cassoux, R. L. Kuczkowski, P. S. Bryan, R. C. Taylor, *Inorg. Chem.* **1975**, *14*, 126 – 129.
[7] a) C. T. Yim, D. F. R. Gilson, *Can. J. Chem.* **1970**, *48*, 515 – 521; b) L. Latanowicz, E. C. Reynhardt, *J. Magn. Reson. Ser. A* **1996**, *121*, 23 – 32; c) G. H. Penner, B. Zhao, K. R. Jeffrey, *Z. Naturforsch. A* **1995**, *50*, 81 – 89.
[8] S. Aldridge, A. J. Downs, C. Y. Tang, S. Parsons, M. C. Clarke, R. D. L. Johnstone, H. E. Robertson, D. W. H. Rankin, D. A. Wann, *J. Am. Chem. Soc.* **2009**, *131*, 2231 – 2243.
[9] a) A. K. Jonscher, *Nature* **1977**, *267*, 673 – 679; b) D. P. Almond, C. R. Bowen, *Phys. Rev. Lett.* **2004**, *92*, 157601.
[10] Y. Liu, Y. Zhang, M.-J. Chow, Q. N. Chen, J. Li, *Phys. Rev. Lett.* **2012**, *108*, 078103.
[11] H. Khanbareh, J. B. J. Schelen, S. van der Zwaag, W. A. Groen, *Rev. Sci. Instrum.* **2015**, *86*, 105111.
[12] Y. Rakita, E. Meirzadeh, T. Bendikov, V. Kalchenko, I. Lubomirsky, G. Hodes, D. Ehre, D. Cahen, *APL Mater.* **2016**, *4*, 051101.
[13] C. R. Bowen, J. Taylor, E. LeBoulbar, D. Zabek, V. Topolov, *Mater. Lett.* **2015**, *138*, 243 – 246.
[14] a) C. R. Bowen, H. A. Kim, P. M. Weaver, S. Dunn, *Energy Environ. Sci.* **2014**, *7*, 25 – 44; b) P. Martins, J. S. Nunes, G. Hungerford, D. Miranda, A. Ferreira, V. Sencadas, S. Lanceros-Méndez, *Phys. Lett. A* **2009**, *373*, 177 – 180.
[15] Y. Zhang, Y. Bao, D. Zhang, C. R. Bowen, *J. Am. Ceram. Soc.* **2015**, *98*, 2980 – 2983.
[16] I. Hatta, A. Ikushima, *J. Phys. Soc. Jpn.* **1976**, *41*, 558 – 564.
[17] J. I. Roscow, Y. Zhang, M. J. Kraśny, R. W. C. Lewis, J. Taylor, C. R. Bowen, *J. Phys. D* **2018**, *51*, 225301.

Manuscript received: February 4, 2020
Accepted manuscript online: February 27, 2020
Version of record online: March 19, 2020

